KERNFORSCHUNGSANLAGE JÜLICH
GESELLSCHAFT MIT BESCHRÄNKTER HAFTUNG

Institut für Reaktorentwicklung

Dose Rate Calculations for a Fusion Ignition Experiment

by

H. Brockmann and U. Ohlig

Jül - 1268
Februar 1976

Als Manuskript gedruckt

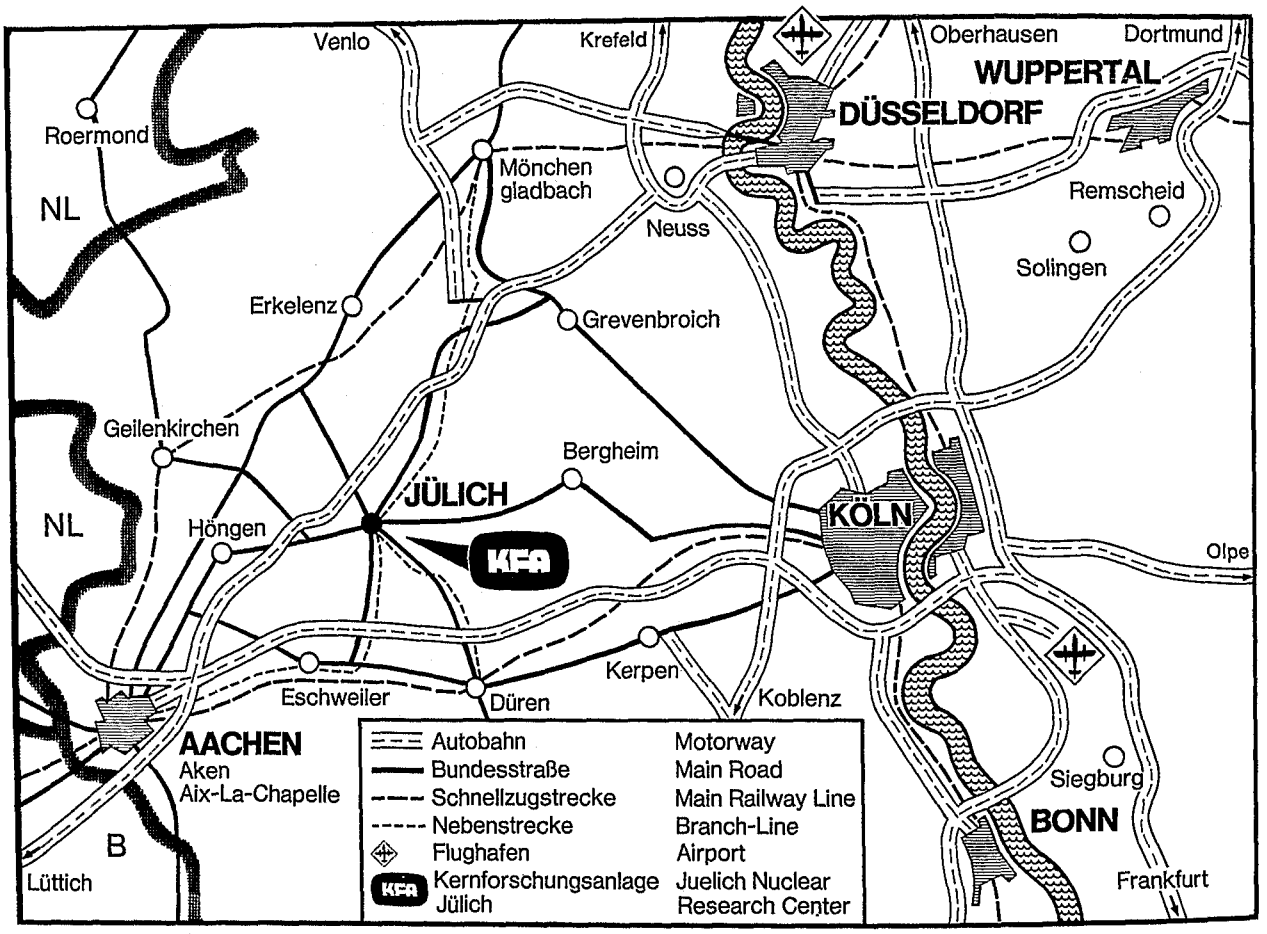

Berichte der Kernforschungsanlage Jülich – Nr. 1268

Institut für Reaktorentwicklung Jül - 1268

Im Tausch zu beziehen durch: ZENTRALBIBLIOTHEK der Kernforschungsanlage Jülich GmbH, Jülich, Bundesrepublik Deutschland

Dose Rate Calculations for a Fusion Ignition Experiment

by

H. Brockmann and U. Ohlig

This work has been performed under EUR-JET study contract No. C 91-GK-30

Kernforschungs-
anlage Jülich
GmbH IRE

JÜL - 1268

February 1976

Dose Rate Calculations for a Fusion Ignition Experiment*

by

H. Brockmann
U. Ohlig

ABSTRACT

In the next generation of fusion experiments, which are planned to reach thermonuclear ignition conditions, a deuterium-tritium mixture will be used as fuel. If significant D-T burning is achieved in these devices a large number of 14.1 MeV neutrons will be produced which will activate the components used in the experiments. The resulting activation radiation will create additional problems of access to the machine for maintenance and repair, which should be taken into account in the design and construction phase of these experiments. To give an idea of the dose rates to be expected, some activation calculations for a typical large Tokamak ignition experiment are presented. It is assumed that the machine is operated in a pulsed mode at an average of 100 plasma discharges within one week and that 10^{20} neutrons per pulse are produced.
The investigation shows that 30 days after shutdown of the machine the total absorbed dose rate in the vicinity of the device is about 0.2 rem/h which limits the working time in this area to about 10 h per quarter. For repairs inside the vacuum vessel or dismantling of the machine it is assumed that the machine can be divided into eight identical segments. The dose rates from an isolated segment and from the remaining part of the machine after removal of one segment are calculated. The results for both cases are of the same order of magnitude and are in the range of 2 to 4 rem/h for decay times between 5 and 30 days. Hence, all repairs inside the vacuum vessel or dismantling of the machine must be done by remote control.

* This work has been performed under EUR-JET study contract No. C 91-GK-30.

CONTENTS

1. INTRODUCTION

Fusion experiments have been operated so far using hydrogen, deuterium or other gases under conditions precluding any appreciable neutron emission from nuclear reactions. However, in the next generation of experiments, which are planned to achieve thermonuclear ignition conditions, a deuterium-tritium mixture will be used as fuel. If significant D-T burning is reached in these devices, a large number of 14.1 MeV neutrons will be produced which will activate the machine components surrounding the plasma, such as the vacuum vessel, the magnetic field coils, and the internal diagnostic equipment. The activation radiation will create additional problems of access to the machine for maintenance and repair which have to be taken into account in the design and construction phase of these experiments. The resulting dose rates will depend upon the number of neutrons produced, upon the chemical composition of the materials used, and to a smaller extent upon the geometry of the machine. To give an idea of the dose rates to be expected some activation calculations for a typical large Tokamak ignition experiment are presented.

2. TECHNICAL DESCRIPTION OF THE EXPERIMENT

The experiment considered is an air-cored Tokamak device with a low aspect ratio. The main components of the machine are 16 copper toroidal field coils (B_Φ), a stainless steel vacuum vessel,

and copper ohmic heating (B_θ) and vertical field coils (B_v) which are situated between the vacuum vessel and the toroidal field coils. In the calculations, the ohmic heating coils which produce the plasma current and the vertical field windings which maintain the toroidal equilibrium of the plasma were approximated by two semicircular copper shells having radial thicknesses of 8.3 and 5.6 cm respectively. The windings are encased in a 2.8 cm thick glass fibre-reinforced epoxy resin insulation. The configuration and dimensions of the machine are shown in Fig. 1. The densities and compositions of the materials used are given in Table I. To make provision for shielding of the area adjacent to the experiment from the neutrons produced during each plasma discharge and from the resulting gamma radiation, the machine is located inside a shielding blockhouse. In the calculations, it was assumed that the experiment is operated in a pulsed mode at an average of 1oo shots per week and that $1o^{2o}$ neutrons per pulse are produced.

3. METHODS USED FOR THE COMPUTATION OF THE DOSE RATE

The dose rate from the components of the machine was calculated by two different methods: by a combined neutron and gamma-ray transport calculation; and by a point kernel integration using dose build-up factors to take into account the multiple scattering of the gamma-rays.

In the combined neutron and gamma-ray transport calculations, the toroidal machine was approximated by a set of infinitely long

cylindrical shells disregarding the contribution of the B_Φ-coils. The screening of the radiation by the B_Φ-coils did not need to be considered since most of the radiation observed at the point of interest does not pass through the B_Φ-coils. The concrete shield surrounding the machine was approximated by a 2 m thick cylindrical shell having the same axis as the vacuum vessel. The inner radius of the shield was 7.48 m. The space- and energy-dependent neutron and gamma-ray fluxes were determined by the one-dimensional discrete-ordinates transport code ANISN (1).

The above procedure does not yield the individual dose contributions of the various components of the machine. To determine these, the dose rate was computed using the point kernel integration method by multiplying the point kernel for the uncollided dose rate by dose build-up factors. This is decribed by the formula

$$P(\vec{r}) = \sum_g \int_V B(\tau^g) \frac{U^g \times S^g(\vec{r}') e^{-\tau^g}}{4\pi |\vec{r} - \vec{r}'|^2} \, d\vec{r}'$$

with

$\vec{r}$ = position of the detector point

$\vec{r}'$ = coordinate of the source point

$d\vec{r}'$ = volume element around $\vec{r}'$

$P(\vec{r})$ = dose rate at the detector point

$S^g(\vec{r}')$ = gamma source for group g (photons/cm^3-sec)

U^g = conversion factor from gamma-ray flux to absorbed dose rate

$\tau^g = \int d\,s\,\mu^g(s)$ = optical path length between source point and detector point

μ^g = linear attenuation coefficient for group g

$B(\tau^g)$ = dose build-up factor

V = volume of the component considered

The space- and energy-dependent gamma-ray sources $S^g(\vec{r}')$ were determined by the code ANISN for the geometry described above.

The method also allows one to compute the dose rate from the B_Φ -coils by making some approximations with regard to the distribution of the gamma-ray sources in these components. It was assumed that the source strength at the inner side of the B_Φ-coils is equal to the source strength at the outer surface of the equivalent $B_{\Theta,V}$-coil and that the radial dependence of the source strength in the two coils is nearly the same.

4. NEUTRON AND GAMMA-RAY DATA

In the main, three types of nuclear data are of importance for the dose-rate calculations: neutron cross sections, which determine the neutron transport; gamma-ray production cross sections; and photon data which describe the transport of the gamma-rays generated in the machine. The neutron cross sections for the materials of interest were taken from the ENDF/B-3 data file (2). The group cross sections and scattering matrices were generated by the code SUPERTOG (3). Neutron activation cross sections not given in the ENDF/B data file were compiled from a

literature study based on the Computer Index of Neutron Data (CINDA) (4).

The radionuclides considered in the dose rate calculations are listed in Table II. The half-lives, energies and intensities of the emitted photons were taken from the literature (5). A code was written to process the activation cross sections and the energies and intensities of the photons into time-dependent activation gamma-ray spectra, assuming that the angular distribution of the emitted photons is isotropic.

The photon group constants and the group-to-group transfer cross sections were calculated by the code MUG (6) using the DLC-7 photon interaction library (7). The dose build-up factors for iron and concrete were taken from the Reactor Shielding Design Manual (8). Since no values could be found in the literature for copper, the values for iron were used. This is justified since the atomic numbers of the two elements are nearly the same. The neutron and gamma-ray interaction cross sections as well as the gamma-ray production data were combined into a coupled cross section library, with the gamma-ray production data appearing as transfer cross sections in a scattering matrix which contains the neutron and photon energy groups.

5. RESULTS AND DISCUSSION

In the first series of calculations the dose rate was determined at a detector point lying between two adjacent B_ϕ-coils on the median plane of the machine (Fig. 1). The radial

distance of the detector point from the plasma centerline was 2.48 m. The radiation attenuation by the glass fibre/epoxy zones was neglected in the dose rate calculations to compensate to some extent for the excessive attenuation which is inherent in approximating the B_Θ- and B_V-coils by a uniform shell.

A second series of calculations has been made to study the problems which will arise if,due to internal damage of the vacuum wall, repairs inside the vacuum vessel become necessary and the assembly has to be dismantled. For the sake of dismantling it was assumed that the machine can be divided into eight identical modules. To estimate the dose rate from an isolated module, the radiation from a cylindrical piece of 2 m in length, equivalent to the mean length of a torus segment, was considered. The dose rate was determined at a point on the axis of the cylinder and at o.5 m from its end surface. In addition, the dose rate from the remaining parts of the machine was assessed with one segment removed.
In this case, the point of interest was located on the plasma centerline in the middle of the resulting gap. Due to the curvature of the machine, this point can only be reached by radiation from those parts of the torus which are within an axial distance of about 3 m. Therefore, the dose rate was calculated from two straight cylindrical pieces which were 3 m long and whose end surfaces were 2 m distant from each other. The detector point was located halfway between the two cylinders.

The energy- and space-dependent neutron and gamma-ray fluxes were determined in the P_3, S_8 approximation. The plasma in the interior of the machine was considered to be an isotropic and homogeneous source of 14.1 MeV neutrons. Multiplication of the gamma-ray fluxes at the detector point by appropriate conversion factors gives the desired absorbed dose rate, which was determined for selected times after 1oo plasma discharges within one week. In addition, the dose rate from the various components of the machine was calculated by the point kernel integration method using the energy- and space-dependent gamma sources determined in the above computer runs. Except for the concrete shield, a 4 m long cylinder was considered, since the contribution from the more distant parts could be neglected. Due to self-shielding only the two B_Φ-coils near the detector point needed to be considered in the calculation. Since the attenuation of the radiation by the concrete is smaller than by the machine components, the contribution from a 1o m long cylinder was considered in this case.

For a comparison of the two calculational methods, the total absorbed dose rates are given in Table III neglecting the contribution from the B_Φ-coils. Except for the first time step, the results from both methods agree well. The ANISN results calculated with the combined library are about 3 - 7 % higher than the values determined by the point kernel method, which is tolarable for this kind of calculation. The absorbed dose rates from the individual components are plotted in Fig. 2 as a function of the decay time. Within 5 days after the 1oo discharges, the

active short-lived radionuclides have decayed and the dose rate decreases rapidly. After this time only a few long-lived radionuclides determine the dose rate and the time dependence is correspondingly smoother. Up to about 14o days, the main part of the radiation is due to the vacuum vessel, despite the fact that it is screened by the 5.6 cm thick equivalent copper coil. The radiation from the vacuum vessel originates primarily from the radionuclides ^{54}Mn, ^{51}Cr, ^{59}Fe, ^{58}Co, and ^{6o}Co. After about 14o days, the equivalent $B_{\Theta,v}$-coil gives the main contribution to the total dose rate, which is primarily due to the ^{6o}Co isotope. Because of its long half-live of 5.26 years, the dose rate from this component is nearly constant over the time considered. The same holds true for the B_{Φ}-coils, but the resulting values are about one order of magnitude lower. The contribution from the concrete shield is the smallest and the radiation is primarily determined by the radionuclides ^{54}Mn, ^{51}Cr, ^{59}Fe and ^{22}Na.

For the case where no special shield is employed to reduce the activation of the components and to absorb the gamma radiation, the machine is so radioactive several hours after shutdown that remote handling techniques are required. After a decay time of 3o days the resulting dose rate is still about o.2 rem/h, and according to the basic safety standard for radiation protection (9) a worker would not be permitted to work for more than 1o hours per quarter in the vicinity of the machine. The situation becomes even more difficult if repairs inside the vacuum vessel, or dismantling of the machine, be-

comes necessary. To illustrate this, the total dose rates from an isolated torus segment and from the remaining parts of the machine after removal of one segment are shown in Table IV. In these two cases, the contribution from the vacuum vessel dominates and the portions of the toroidal field coils and the shielding can be neglected. Allowing for a reasonable decay time of 5 to 3o days between the damage and repair of the machine, the resulting dose rate lies between 2 and 4 rem/h. Thus, it follows that after only 1oo plasma discharges within one week the machine becomes so radioactive that remote handling techniques are required in order to make major modifications to the experiment or to repair the machine if a section of the vacuum vessel is damaged.

6. CONCLUSIONS

The objective of this analysis is to determine the activation of the components of future fusion experiments and to assess the resulting dose rates if these experiments are operated with a deuterium-tritium mixture under ignition conditions. The calculations were made for a typical Tokamak device assuming that the experiment is operated in a pulsed mode at an average of 1oo shots per week and that $1o^{2o}$ neutrons per pulse are produced.

The investigation shows that several hours after shutdown the machine is so radioactive that remote handling techniques are necessary if work has to be done at the machine. After 3o days, which may still be a reasonable decay-time with regard to repairs, the dose rate between two adjacent B_ϕ-coils on the me-

dian plane of the machine is about o.2 rem/h. In this case a worker is permitted to work for only about 1o hours per quarter in the vicinity of the machine. The resulting activation radiation can be reduced if a radiation shield is employed and the influence of a shield should be studied in further calculations. But even if an additional shield is employed, remote handling equipment is required in case either repairs inside the vacuum vessel or dismantling of the machine become necessary. Assuming that the toroidal machine can be divided into eight identical modules, the absorbed dose rates from an isolated segment and from the remaining parts of the machine were calculated. The resulting values are of the same order of magnitude for both cases considered. For decay-times between 5 and 3o days the dose rate is still in the range of 2 to 4 rem/h so that all work inside the vessel needs to be done by remote control.

7. REFERENCES

(1) Engle, W.W., jr., A User's Manual for ANISN, Report K-1693, Union Carbide Corporation (1967).

(2) Drake, M.K. (Ed.), Data Formula and Procedures for the ENDF Neutron Cross Section Library, Brookhaven National Laboratory, BNL-5o274 (T - 6o1) (197o).

(3) Wright, R.A., et al., SUPERTOG-3 Data Generator: Fine Group Constants and P_n Scattering Matrices from ENDF/B, ORNL-TM-2679 (1972).

(4) An Index to the Literature on Microscopic Neutron Data (CINDA 1975), International Atomic Energy Agency (1975).

(5) **Erdtmann,G.**, Soyka, W., Die γ- Linien der Radionuklide, Band 1, JÜL-1oo3 AC (1973).

(6) Knight, J.R., Mynatt, F.R., MUG: A Program for Generating Multigroup Photon Cross Sections, CTC-17, Union Carbide Corporation (197o).

(7) HPIC: Evaluated Photon Interaction Library, ENDF/B File 23 Format, DLC-7 (1969).

(8) Rockwell, Th. (Ed.), Reactor Shielding Design Manual, First Edition, MacMillan and Co., London.

(9) Basic Safety Standard for Radiation Protection, Safety Series No. 9, International Atomic Energy Agency, Vienna (1962).

8. FIGURES AND TABLES

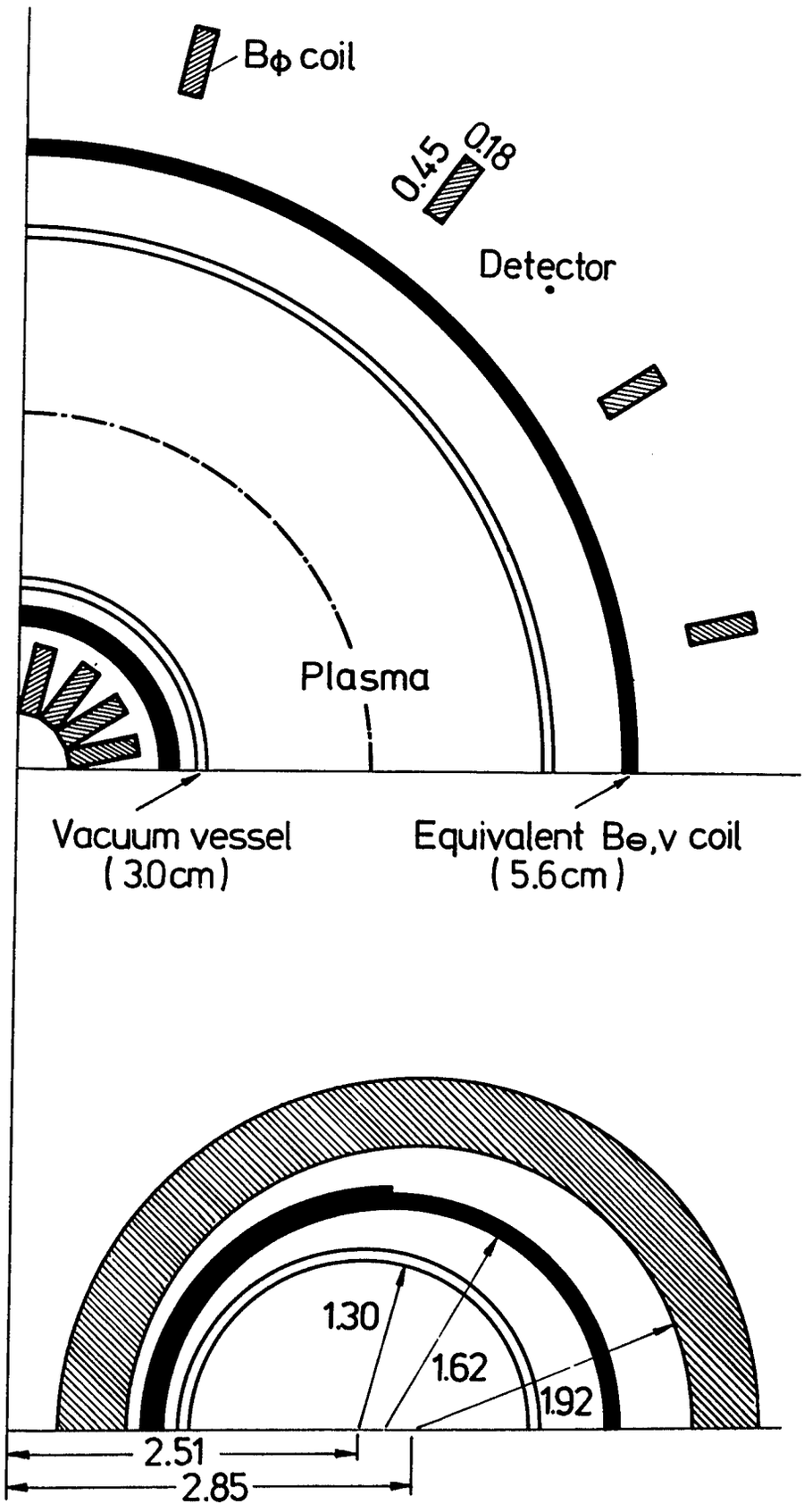

Fig. 1. Top- and side-view of the experimental assembly. All dimensions in metres.

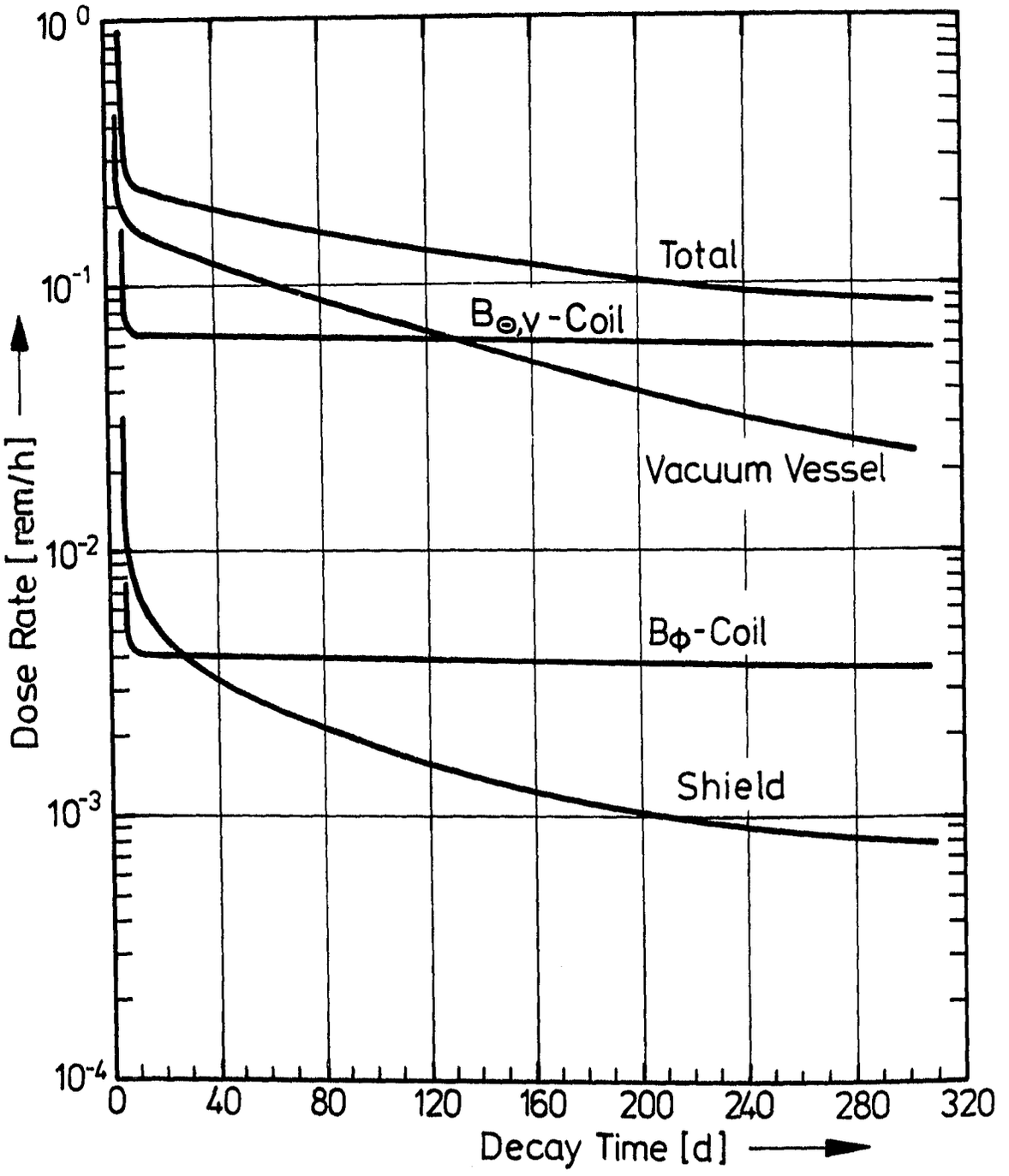

Fig. 2. Time behavior of the absorbed dose rate at a specific point (1oo plasma discharges per week).

TABLE I. SUMMARY OF MATERIAL COMPOSITIONS AND DENSITIES

Material	Composition (weight per cent)
Vacuum Vessel	
Stainless Steel (ρ = 7.9o g/cm^3)	Mn: 2, Ni: 8, Cr: 18, Fe: 72
Magnetic Field Coils	
Copper (ρ = 8.93 g/cm^3)	Cu: 1oo
Insulation	
Glass Fibre (ρ = 2.5o g/cm^3)	SiO_2: 54.5, Al_2O_3: 14.5, CaO : 22.o, B_2O_3 : 8.5, Na_2O: o.5
Epoxy (ρ = 1.3o g/cm^3)	C: 7o.65, H: 6.29, O: 23.o4 N: o.o1
Shield	
Portland Concrete (ρ = 2.3o g/cm^3)	H: 1, O: 53, Si: 34, Al: 3.3, Fe: 1.3, Ca: 4.3 Na: 3.1

TABLE II. ACTIVATION REACTIONS OF INTEREST AND HALF-LIVES OF THE RADIONUCLIDES PRODUCED

Reaction	Half-Life	Reaction	Half-Life
Na-23 (n,2n) Na-22	2.6o a	Ca-48 (n,n'p) K-47[4]	18.o s
Na-23 (n,γ) Na-24	15.o h	Ca-48 (n,2n) Ca-47[2]	4.54 d
Al-27 (n,α) Na-24	15.o h	Cr-5o (n,2n) Cr-49	41.9 m
Al-27 (n,p) Mg-27	9.48 m	Cr-5o (n,γ) Cr-51	27.8 d
Al-27 (n,2n) Al-26	$7.4 \cdot 1o^5$ a	Cr-52 (n,p) V-52	3.75 m
Al-27 (n,γ) Al-28	2.31 m	Cr-52 (n,2n) Cr-51	27.8 d
Si-28 (n,t) Al-26	$7.4 \cdot 1o^5$ a	Cr-53 (n,n'p) V-52	3.75 m
Si-29 (n,2p) Mg-28	21.3 h	Cr-53 (n,p) V-53	1.55 m
Si-3o (n,^{3}He) Mg-28[1]	21.3 h	Cr-54 (n,α) Ti-51	5.79 m
Ca-4o (n,p) K-4o	$1.28 \cdot 1o^9$ a	Mn-55 (n,2n) Mn-54	312.5 d
Ca-42 (n,t) K-4o	$1.28 \cdot 1o^9$ a	Fe-54 (n,α) Cr-51	27.8 d
Ca-42 (n,p) K-42	12.36 h	Fe-54 (n,t) Mn-52	5.6o d
Ca-43 (n,n'p) K-42	12.36 h	Fe-54 (n,t) Mn-52m[5]	21.3 m
Ca-43 (n,p) K-43	22.o h	Fe-54 (n,p) Mn-54	312.5 d
Ca-44 (n,t) K-42	12.36 h	Fe-54 (n,2n) Fe-53	8.51 m
Ca-44 (n,n'p) K-43	22.o h	Fe-56 (n,p) Mn-56	2.58 h
Ca-46 (n,α)) Ar-43[3]	5.4o m	Fe-57 (n,n'p) Mn-56	2.58 h
Ca-46 (n,γ) Ca-47[2]	4.54 d	Fe-57 (n,p) Mn-57	1.54 m

TABLE II. (Continued)

Reaction	Half-Life		Reaction	Half-Life	
Fe-58 (n,α) Cr-55	3.59	m	Cu-63 (n,γ) Cu-64	12.8	h
Fe-58 (n,p) Mn-58	65.3	m	Cu-65 (n,α) Co-62	13.5	m
Fe-58 (n,γ) Fe-59	44.6	d	Cu-65 (n,α) Co-62m	1.5	m
Ni-58 (n,d) Co-57	27o.o	d	Cu-65 (n,p) Ni-65	2.54	h
Ni-58 (n,p) Co-58	71.3	d	Cu-65 (n,2n) Cu-64	12.8	h
Ni-58 (n,2n) Ni-57[6]	36.o	h	Cu-65 (n,γ) Cu-66	5.1	m
Ni-6o (n,p) Co-6o	5.26	a			
Ni-6o (n,p) Co-6om[7]	1o.47	m			
Ni-61 (n,n'p) Co-6o	5.26	a			
Ni-61 (n,n'p) Co-6om[7]	1o.47	m			
Ni-62 (n,α) Fe-59	44.6	d	1) Mg-28 → Al-28	2.31	m
Ni-62 (n,p) Co-62	13.5	m	2) Ca-47 → Sc-47	3.4o	d
Ni-62 (n,p) Co-62m	1.5	m	3) Ar-43 → K -43	22.o	m
Ni-64 (n,α) Fe-61[8]	6.o7	m	4) K- 47 → Ca-47[2]	4.54	d
Ni-64 (n,γ) Ni-65	2.54	h	5) Mn-52m → Mn-52	5.6o	d
Cu-63 (n,α) Co-6o	5.26	a	6) Ni-57 → Co-57	27o.o	d
Cu-63 (n,α) Co-6om[7]	1o.47	m	7) Co-6om → Co-6o	5.26	a
Cu-63 (n,2n) Cu-62	9.73	m	8) Fe-61 → Co-61	1.61	h

TABLE III. COMPARISON OF TOTAL DOSE RATES OBTAINED FROM DIFFERENT METHODS

Decay Time (days)	Absorbed Dose Rate (rem/h) Combined Transport Calculation	Point Kernel Integration
5	$1.02 \cdot 10^{0}$	$8.07 \cdot 10^{-1}$
10	$2.41 \cdot 10^{-1}$	$2.33 \cdot 10^{-1}$
30	$2.08 \cdot 10^{-1}$	$2.02 \cdot 10^{-1}$
70	$1.69 \cdot 10^{-1}$	$1.63 \cdot 10^{-1}$
150	$1.24 \cdot 10^{-1}$	$1.18 \cdot 10^{-1}$
200	$1.08 \cdot 10^{-1}$	$1.02 \cdot 10^{-1}$
250	$9.83 \cdot 10^{-1}$	$9.11 \cdot 10^{-1}$
300	$8.97 \cdot 10^{-1}$	$8.35 \cdot 10^{-1}$

TABLE IV. TOTAL DOSE RATES FROM AN ISOLATED SEGMENT AND FROM THE REMAINING 7/8^{ths} OF THE MACHINE FOR VARIOUS DECAY TIMES AFTER SHUTDOWN

Decay Time (days)	Absorbed Dose Rate (rem/h) Cylinder Segment	Remaining 7/8^{ths} of the Machine
o	$1.24 \cdot 10^{2}$	$1.91 \cdot 10^{2}$
5	$2.73 \cdot 10^{o}$	$4.o3 \cdot 10^{o}$
1o	$2.39 \cdot 10^{o}$	$3.52 \cdot 10^{o}$
3o	$1.97 \cdot 10^{o}$	$2.91 \cdot 10^{o}$
7o	$1.41 \cdot 10^{o}$	$2.o8 \cdot 10^{o}$
1oo	$1.12 \cdot 10^{o}$	$1.61 \cdot 10^{o}$
15o	$7.9o \cdot 10^{-1}$	$1.17 \cdot 10^{o}$
2oo	$5.82 \cdot 10^{-1}$	$8.63 \cdot 10^{-1}$
25o	$4.46 \cdot 10^{-1}$	$6.63 \cdot 10^{-1}$
3oo	$3.55 \cdot 10^{-1}$	$5.26 \cdot 10^{-1}$